

Study of Intermolecular Interaction for the Spin-Crossover Iron(II) Compounds

Shinya Hayami,* Ryo Kawajiri, Gergely Juhász, Takayoshi Kawahara, Koichiro Hashiguchi, Osamu Sato,† Katsuya Inoue,†† and Yonezo Maeda*

Department of Chemistry, Faculty of Sciences, Kyushu University, 6-10-1, Hakozaki, Higashi-ku, Fukuoka 812-8581

†Kanagawa Academy of Science and Technology, East 412, 3-2-1 Sakado, Takatsu-ku, Kawasaki 213-0012

††Institute for Molecular Science, Myodaiji, Okazaki 444-8585

(Received December 27, 2002)

The thermal spin transitions of iron(II) spin-crossover compounds $[Fe(PM\text{-}iPA)_2(NCS)_2]$ (**1**) and $[Fe(PM\text{-}iPA)_2(NCSe)_2]$ (**2**) (PM-iPA = *N*-(2′-pyridylmethyl)-isopropylamine) have occurred at $T_{1/2} = 267$ K and 376 K without thermal hysteresis. No light-induced excited spin state trapping (LIESST) effect was observed for compounds **1** and **2** even at 5 K. The iron(II) spin-crossover compounds $[Fe(PM\text{-}L)_2(NCX)_2]$ (PM-A = *N*-(2′-pyridylmethyl)-aniline, PM-BiA = *N*-(2′-pyridylmethyl)-4-aminobiphenyl, PM-TeA = *N*-(2′-pyridylmethyl)-4-aminoterphenyl, PM-PEA = *N*-(2′-pyridylmethyl)-4-(phenylethynyl)aniline, and PM-AzA = *N*-(2′-pyridylmethyl)-4-(phenylazo)aniline; X = S and Se) with ligands having π-systems have exhibited the LIESST effect, and the critical LIESST temperature, T_c(LIESST), has been observed. The compounds **1** and **2** are crystallized at *Pnna* and $C2/c$ at 298 K, respectively, and the space groups of the compounds remained unchanged until 100 K, although the compounds show the spin transition. The molecular packing structure and thermodynamic parameters of the spin transitions calculated from the magnetic susceptibility curves suggest that compounds **1** and **2** have no strong intermolecular interactions between the complexes, while the compounds with π-system ligands form π–π intra- and intermolecular interactions between the ligands. Our conclusion is that the intermolecular interactions play an important role in trapping a light-induced metastatble state.

A number of spin-crossover compounds have been studied.[1] These compounds are important in the development of electronic devices such as molecular switches. In 1984, Decurtins et al. observed a light-induced low-spin (LS) → high-spin (HS) transition, during which the molecules could be quantitatively trapped in the excited HS state at sufficiently low temperatures.[2] The phenomenon is called light-induced excited spin state trapping (LIESST), the existence of the light-induced HS state for the iron(II) spin-crossover compounds was verified with optical and Mössbauer spectroscopy, and magnetic susceptibility measurements.[2–10] The discovery of this LIESST effect suggested that the spin-crossover compounds could be used as optical switches. In the meantime, a number of iron(II) compounds with light-induced metastable HS states at low temperature have been found.[2–10] Very low temperature is required for trapping the system in the metastable HS state. Above a certain critical temperature defined as T_c(LIESST),[8] the system clears the energy barrier between the two spin states and relaxes to the LS state. Hauser et al. have investigated the dynamics of LIESST effect by using optical spectroscopy.[11,12] In their study, a correlation was observed between the lifetime of the LIESST state and the thermal spin-crossover temperature (T_c).[8] Herber et al. reported that a variable-temperature Fourier transform infrared (VTFTIR) technique could be used in order to determine T_c(LIESST).[13,14] Furthermore, Létard et al. investigated the T_c(LIESST) versus T_c variation for 22 LIESST compounds,[8] and suggested a decrease of T_c(LIESST) as T_c increases,[8,15] in agreement with the inverse-energy-gap law proposed by Hauser.[16] Recently, we proposed that the cooperativity resulting from the intermolecular interaction operates to increase the activation energy for the relaxation processes, enabling the observation of a long-lived metastable HS state after illumination.[17,18] Several iron(II) compounds with π-system ligands have been extensively studied by Létard et al.[6–8,10] The compounds exhibited spin-crossover and LIESST effects; furthermore, the physical properties of the single crystals have also been reported.[6–8,10]

Here, we synthesized two compounds without strong intermolecular interactions: $[Fe(PM\text{-}iPA)_2(NCS)_2]$ (**1**) and $[Fe(PM\text{-}iPA)_2(NCSe)_2]$ (**2**). The single crystals were obtained, and the crystal structures of the compounds were investigated for both the LS and HS state, and the photomagnetic properties were studied. No LIESST effect was observed. The structures of compounds **1** and **2** were compared in detail with those of the compounds $[Fe(PM\text{-}AzA)_2(NCS)_2]$ (**3**) and $[Fe(PM\text{-}AzA)_2(NCSe)_2]$ (**4**) that exhibit the LIESST effect (Scheme 1).[6–8,10] Hence, in order to develop a variety of optically switchable molecular solids, strategies to prevent such a rapid relaxation from a metastable state to a ground state should be developed. We propose the introduction of strong intermolecular interactions in molecular compounds. It is thought that the cooperativity resulting from the intermolecular interaction operates to increase the activation energy for the relaxation processes, enabling the observation of a long-lived metastable HS state after illumination.

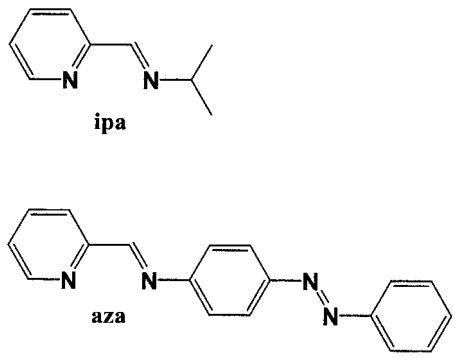

Scheme 1. Chemical structure of the ligands, PM-iPA and PM-AzA.

Experimental

Synthesis. The Schiff-base ligands PM-iPA and PM-AzA were synthesized from the condensation of 2-pyridinecarbaldehyde and isopropylamine or 4-(phenylazo)aniline, respectively. Compound **1** was prepared under nitrogen atomosphere as follows: In 20 mL of distilled methanol were dissolved iron(II) chloride tetrahydrate, $FeCl_2 \cdot 4H_2O$ (0.20 g, 1 mmol), and potassium thiocyanate, KNCS (0.19 g, 2 mmol), in the presence of some crystals of ascorbic acid to prevent iron(II) oxidation. The colorless solution of $Fe(NCS)_2$ was separated from the white precipitate of potassium chloride by filtration and added dropwise to a stoichiometric amount of PM-iPA (0.30 g, 2 mmol) in 20 mL of methanol. Immediately, a violet precipitate of $[Fe(PM\text{-}iPA)_2(NCS)_2]$ (**1**) was formed. It was filtered off, washed several times with diethyl ether, and dried in vacuo. Anal. Calcd for $C_{20}H_{24}N_6S_2Fe$ (**1**): C, 51.28; H, 5.16; N, 17.94. Found: C, 51.37; H, 5.28; N, 18.03. The compounds $[Fe(PM\text{-}iPA)_2(NCSe)_2]$ (**2**), $[Fe(PM\text{-}AzA)_2(NCS)_2]$ (**3**) and $[Fe(PM\text{-}AzA)_2(NCSe)_2]$ (**4**) were prepared in a similar manner by use of an appropriate Schiff-base, and NCS^- or $NCSe^-$ ions. Anal. Calcd for $C_{20}H_{24}N_6Se_2Fe$ (**2**): C, 42.73; H, 4.30; N, 14.95. Found: C, 42.97; H, 4.38; N, 15.02. Anal. Calcd for $C_{38}H_{28}N_{10}S_2Fe$ (**3**): C, 61.29; H, 3.79; N, 18.81. Found: C, 60.96; H, 3.97; N, 18.61. Anal. Calcd for $C_{38}H_{28}N_{10}Se_2Fe$ (**4**): C, 54.43; H, 3.37; N, 16.71. Found: C, 54.93; H, 3.38; N, 16.87.

Physical Measurements. Elemental analyses were performed by the Elemental Analysis Center, Kyushu University. The magnetic susceptibilities $\chi(T)$ for the compounds **1**–**4** were measured between 100 and 400 K with a superconducting quantum interference device (SQUID) magnetometer (Quantum Design MPMS-5S) in an external field of 0.5 T. The Mössbauer spectra (isomer shift vs metallic iron at room temperature) were measured using a constant-acceleration spectrometer (Austin Science Associates (ASA)). The Mössbauer spectrometer with a $^{57}Co/Rh$ source was driven in the transmission mode. The measurements at low temperature were performed with a closed-cycle helium refrigerator (Iwatani Co., Ltd.). LIESST experiments were carried out using a Hg-Xe lamp ($\lambda \approx 550$ nm, 1.5 mW/cm^2) through IR and green filters; the light was guided via an optical fiber into the SQUID. The sample was placed over the edge of the optical fiber.

Crystallographic Data Collection and Structure Determination. Selected violet block crystals of **1** and **2** were mounted in glass capillaries. All measurements were made on a Rigaku RAXIS-RAPID Imaging Plate diffractometer with graphite monochromated Mo-Kα radiation. The data were collected to a maximum 2θ value of 55.0°. The temperature of the crystal was slowly decreased from 298 K to 90 K, and the X-ray structure analyses were carried out at 298 K and 90 K. For **1** at 298 K, of the 17556 reflections which were collected, 2683 were unique and 900 with $I > 3\sigma(I)$ were used to solve the structure with SIR92. For **1** at 90 K, of the 22975 reflections which were collected, 2559 were unique and 1377 with $I > 3\sigma(I)$ were used to solve the structure with SIR92. For **2** at 298 K, of the 9339 reflections which were collected, 2624 were unique and 1107 with $I > 3\sigma(I)$ were used to solve the structure with SIR92. For **2** at 90 K, of the 9400 reflections which were collected, 2560 were unique and 1459 with $I > 3\sigma(I)$ were used to solve the structure with SIR92. Pertinent crystallographic parameters are summarized in Table 1.

Table 1. Crystal Parameters for the Compounds **1** and **2**

Compound	**1**		**2**	
Temperature	298 K	90 K	298 K	90 K
Formula	$C_{20}H_{24}N_6S_2Fe$		$C_{20}H_{24}N_6Se_2Fe$	
Formula weight	468.42		562.22	
Crystal system	orthorhombic		monoclinic	
Space group	*Pnna* (#52)		*C*2/*c* (#15)	
a/Å	16.052(2)	15.845(2)	16.316(1)	16.190(2)
b/Å	13.733(1)	13.275(2)	10.4879(4)	10.406(2)
c/Å	10.552(1)	10.588(2)	15.1863(7)	16.273(2)
β/°			117.011(4)	125.309(3)
V/Å^3	2326.1(8)	2227.1(9)	2315.2(3)	2237.3(5)
Z	4	4	4	4
*R*1	0.051	0.046	0.047	0.045
R	0.094	0.046	0.083	0.075
R_w	0.122	0.052	0.110	0.103

Results and Discussion

Description of the Structure. The crystal structures of **1** and **2** were determined by X-ray diffraction at 298 K and 90 K. The space groups (*Pnna* for **1** and *C*2/*c* for **2**) are retained upon the cooling; there is no crystallographic transition between 298 K and 90 K for **1** or for **2**. Figures 1 and 2 show the ORTEP views of the molecules together with the labelling of the atoms included in the asymmetric unit for **1** and **2**, respectively. The Fe–N(CS) and Fe–N(CSe) distances are shorter than the Fe–N(pyridine and imine) distances. Each iron atom is surrounded by six nitrogen atoms belonging to two NCS^- (or $NCSe^-$) groups in *cis* position and two PM-iPA ligands. The bond lengths and angles at 298 K and 90 K are listed in Table 2. The volume of the unit cell for **1** decreases by 4.26% upon cooling from 298 K to 90 K. The cell parameters *a* and *b* decrease with the decrease in temperature. On the other hand, the third one, *c*, increases significantly. The volume of the unit cell for **2** decreases by 3.36% upon cooling from 298 K to 90 K; the cell parameters *a* and *b* decrease, and the third one, *c*, increases. However, there is no spin transition in the compound **2** between 298 and 90 K; **2** is in the LS state at both temperature.

High-Spin Crystal Structure of 1. The molecular structure of **1** in HS state is shown in Fig. 1 (a). The coordination moiety of the iron is symmetrical. The Fe–N bond lengths and the angles are strongly distorted; the maximum difference is

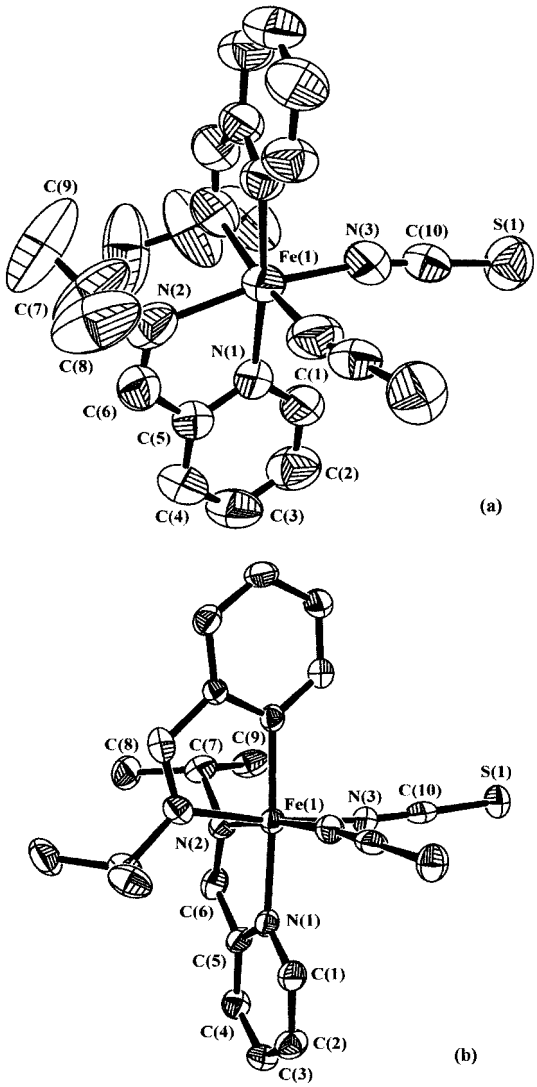

Fig. 1. ORTEP view of $[Fe(PM\text{-}iPA)_2(NCS)_2]$ (**1**) at 298 K (a) and 100 K (b) showing 50% probability displacement ellipsoids. All hydrogen atoms are omitted for clarity.

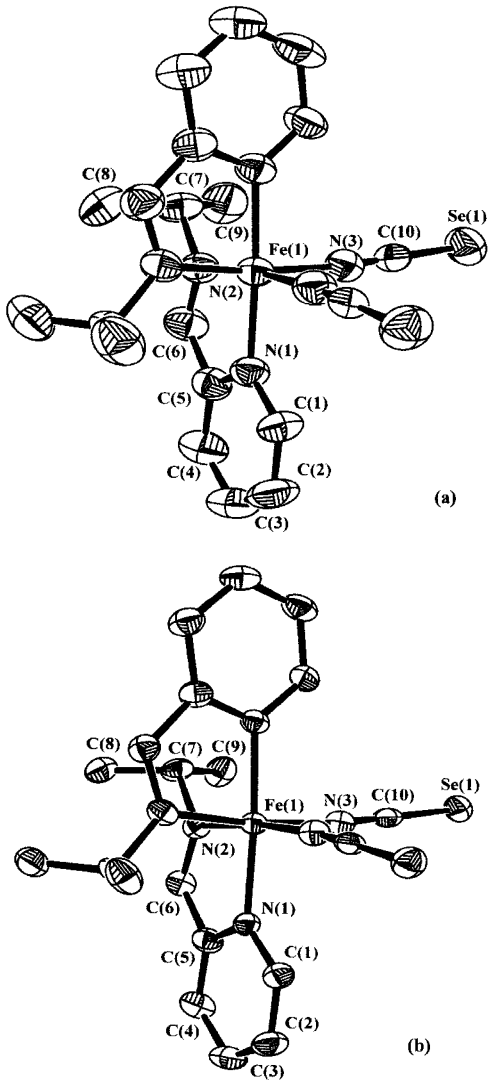

Fig. 2. ORTEP view of $[Fe(PM\text{-}iPA)_2(NCSe)_2]$ (**2**) at 298 K (a) and 100 K (b) showing 50% probability displacement ellipsoids. All hydrogen atoms are omitted for clarity.

ca. 0.10 Å among the Fe–N(CS) (2.050(7) Å), the Fe-N(PM-iPA) (2.151(6) Å (pyridine) and 2.136(6) Å (imine)) bonds. The NCS^- groups are linear (179.1(7)°) and the angle between the two NCS ligands is 91.6(4)°. It can be noticed that the Fe–N–C(S) linkages are slightly bent (168.3(6)°). This is also illustrated by the differences between the N–Fe–N angles: N(1)–Fe–N(1)* = 174.3(3)°, N(2)–Fe–N(3) = 166.7(2)° (Table 2). The dihedral angle between the pyridine ring and the least square plane of the chelate ring (Fe–N(1)–C(5)–C(6)–N(2)) in PM-iPA ligand is 0.050°.

Low-Spin Crystal Structure of 1. The structure of **1** at 90 K is quite similar to that at 298 K, however the spin transition affects principally the geometry of the FeN_6 core. The Fe–N(CS) bond distance is equal to 1.951(4) Å and the Fe–N(pyridine) bond distances are equal to 1.996(4) Å and the Fe–N(imine) distances to 1.946(4) Å. The Fe–N(pyridine) bonds in the LS form are 0.156 Å shorter than those in the HS form: the Fe–N(imine) bonds are shorter by 0.183 Å and the Fe–N(CS) bonds by 0.103 Å than the respective ones in the HS

Table 2. Selected Bond Distances (Å) and Angles (°) for the Compounds **1** and **2**

Compound	**1**		**2**	
Temperature	298 K	90 K	298 K	90K
Fe–N(1)	2.151(6)	1.996(4)	1.989(5)	1.984(4)
Fe–N(2)	2.136(6)	1.946(4)	1.959(6)	1.957(5)
Fe–N(3)	2.050(7)	1.951(4)	1.947(8)	1.941(6)
N(1)–Fe–N(1*)	174.3(3)	177.0(2)	177.0(4)	176.6(3)
N(1)–Fe–N(2)	76.2(2)	81.0(2)	81.0(2)	81.2(2)
N(1)–Fe–N(2*)	99.8(2)	97.0(2)	96.9(2)	96.4(2)
N(1)–Fe–N(3)	91.5(2)	90.2(2)	89.7(2)	90.4(2)
N(1)–Fe–N(3*)	92.5(2)	92.0(2)	92.4(3)	92.0(2)
N(2)–Fe–N(2*)	92.6(3)	92.4(2)	90.2(4)	90.6(3)
N(2)–Fe–N(3)	89.2(2)	90.1(1)	89.9(3)	89.7(2)
N(2)–Fe–N(3*)	167.7(2)	172.7(2)	173.3(2)	173.2(2)
N(3)–Fe–N(3*)	91.6(4)	88.2(2)	90.7(4)	90.9(3)

form. That the decrease observed for Fe–N(PM-iPA) is larger than that for Fe–N(CS) can be accounted for by the fact that PM-iPA ligand is a stronger π-electron acceptor than NCS. The FeN_6 core is less distorted in the LS state than in the HS state. The transition from HS to LS induces the increases $+2.7^\circ$ for N(1)–Fe–N(1)* $= 177.0^\circ$, $+5.0^\circ$ for N(2)–Fe–N(3)* $= 172.7^\circ$ and $+5.0^\circ$ for N(3)–Fe–N(2)* $= 172.7^\circ$ angles. The NCS^- groups are almost linear ($179.2(4)^\circ$) and the angle between the two NCS ligands is $88.2(2)^\circ$. The Fe–N–C(S) linkages are slightly bent ($171.4(4)^\circ$). Furthermore, the bond length, 1.175(6) Å observed for N–C(S) and 1.631(5) Å for (N)C–S bond in the LS form increase to 1.143(8) Å and 1.608 (8) Å in the HS form, respectively.

The compound **2** is in the LS state at both temperatures; therefore, no comparison of the structure in the HS and the LS states is possible.

Magnetic Properties. The temperature dependences of the magnetic susceptibility for **1** and **2** were measured at a rate of 2 K min^{-1} in the form of the $\chi_m T$ versus T curve, where χ_m is the molar magnetic susceptibility and T is the temperature. $T_{1/2}\downarrow$ and $T_{1/2}\uparrow$ are defined as the inversion temperatures at which there are 50% of HS and 50% of LS molecules in the cooling and warming modes, respectively. The magnetic properties of the compounds **1** and **2** are represented in Figs. 3(a), (b), respectively. The compounds **1** and **2** exhibit spin-crossover behavior. At 100 K, $\chi_m T$ for **1** is close to 0 cm^3 K mol^{-1}, which is in the range of values expected for LS iron(II) ions. The $\chi_m T$ value at 400 K was 3.38 cm^3 K mol^{-1}; the spin transition occurs gradually in the temperature range from 200 to 350 K with around $T_{1/2}\uparrow = 270$ K. On cooling, the $\chi_m T$ value decreased with decrease in temperature and $T_{1/2}\downarrow = 270$ K was obtained, showing that the HS moieties were restored to one of the LS states without any thermal hysteresis loop. The compound **2** also exhibits a gradual spin-crossover with $T_{1/2}\uparrow = T_{1/2}\downarrow = 375$ K without any thermal hysteresis loop. Létard et al. have reported that the compounds **3** and **4** have exhibited gradual spin-crossover behavior and that $T_{1/2}$ for **3** and **4** are 184 and 255 K without any thermal hysteresis loop, respectively.[6–8,10] In general, the compounds with NCSe anion ligands experience spin transition at higher temperatures than those with NCS, because of the vibration mode of the heavy atoms. The spin transition temperature of **2** is 105 K higher than that of **1**, and the spin transition temperature of **4** is 71 K higher than that of **3**.

Mössbauer spectra for **1** and **3** were measured at 293 K and 80 K, and are shown in Figs. 4 and 5, respectively; two doublets (d1 and d2) were observed for **1** at 293 K. The d1 doublet has a quadrupole splitting $Q.S. = 2.27$ mm s^{-1} and isomer shift $I.S. = 1.34$ mm s^{-1}, of which the parameters correspond to the HS state of iron(II) compounds; the d2 doublet has a quadrupole splitting $Q.S. = 0.38$ mm s^{-1} and isomer shift $I.S. = 0.19$ mm s^{-1} corresponding to the LS state of iron(II) compounds. A doublet with $Q.S. = 0.65$ and $I.S. = 0.49$ mm s^{-1} corresponding to the LS state of iron(II) compounds was observed for **1** at 80 K. A small absorption is noted in the spectrum at 80 K; this can be ascribed to one component of a minority impurity. A doublet was observed in the Mössbauer spectrum at 293 K for **3** and was assigned to the HS state of iron(II) compounds; the values of fitted parameters are

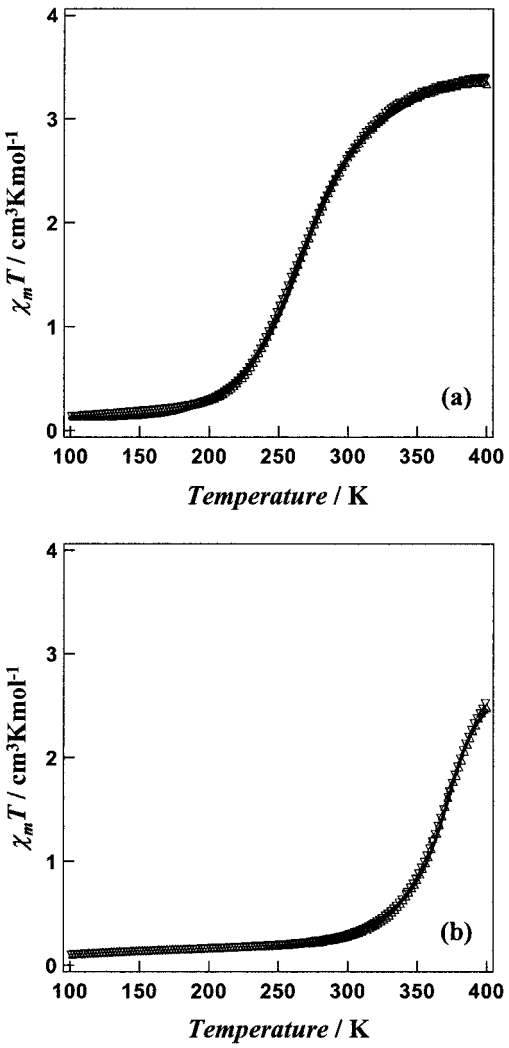

Fig. 3. Experimental and simulated $\chi_m T$ versus T plots for **1** (a) and **2** (b). Sample was warmed from 100 K to 400 K at a rate of 2 K min^{-1}. The simulated curves are in full lines (see text and Eq. 1).

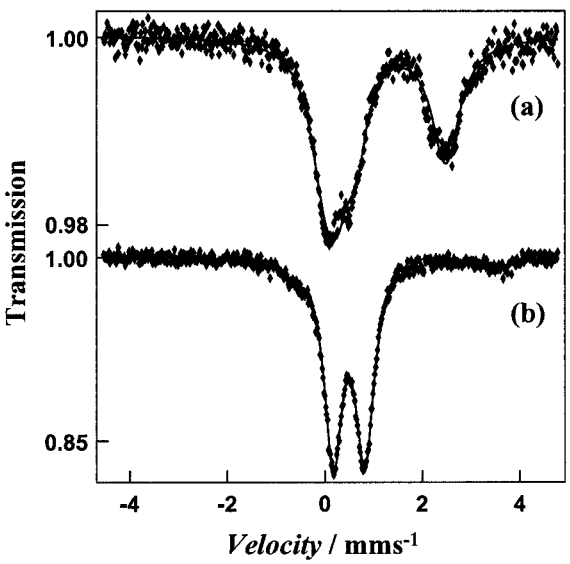

Fig. 4. Mössbauer spectra of **1** at 293 K (a) and at 80 K (b).

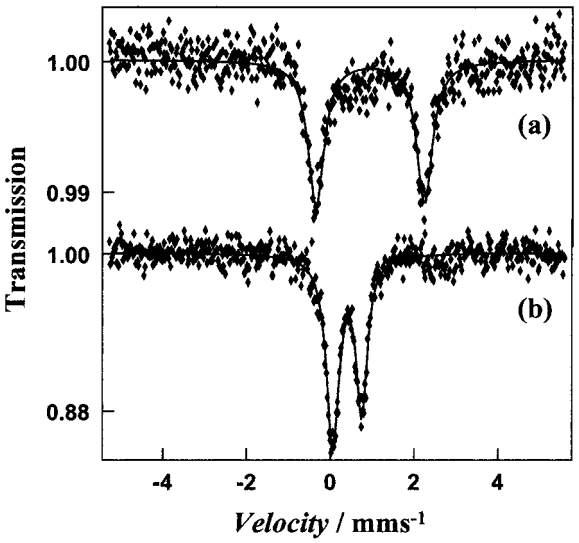

Fig. 5. Mössbauer spectra of **3** at 293 K (a) and at 80 K (b).

$Q.S. = 2.60\ \mathrm{mm\,s^{-1}}$ and $I.S. = 0.95\ \mathrm{mm\,s^{-1}}$. A doublet with $Q.S. = 0.69\ \mathrm{mm\,s^{-1}}$ and $I.S. = 0.40\ \mathrm{mm\,s^{-1}}$ corresponding to the LS state of iron(II) compounds was observed at 80 K for **3**. A small doublet was observed as a minority impurity at 80 K for **3**. The temperature dependence of the ratios of the HS to the LS populations calculated from the absorption area in the Mössbauer spectra agrees with that obtained from the magnetic susceptibility. The Mössbauer spectra for **2** and **4** could not be observed because of the shielding effect of selenium atoms.

The magnetic behavior after light irradiation was recorded for compounds **1** and **2** in order to investigate the photomagnetic properties. A Hg-Xe lamp ($\lambda \approx 550$ nm, $1.5\ \mathrm{mW\,cm^{-2}}$) was used as a light source in the investigation of illumination effects. The light passes through IR and green filters, and was guided via an optical fiber into the SQUID. The sample was placed over the edge of the optical fiber. When the sample was illuminated at 5 K, an increase in the dc susceptibility was observed for **3** and **4**. The change in the magnetization persisted for many hours, even after the illumination was stopped. This increase suggests that the transition from the LS state to the HS state was induced by the illumination. As Létard et al. have reported photomagnetic properties, the temperature dependence of $\chi_m T$ after irradiation shows that the magnetization decreases with the increase in temperature and the relaxation to the ground state occurs with T_c(LIESST) = 44 K for **3** and 25 K for **4**.[8] When the samples **1** and **2** were illuminated at 5 K, however, no increase in the susceptibility was observed. This fact suggests that the spin-crossover iron(II) compounds **1** and **2** do not exhibit any LIESST effect even at 5 K.

The careful investigation of the intermolecular arrangement of these compounds show that the compounds **1** and **2** do not have any strong intermolecular interactions (Figs. 6(a), (b)). The iron atoms of the compounds **1** and **2** are coordinated by PM-iPA ligand with bulky isopropyl group, and this substitute prevents any strong interactions between complex molecules. The iron atoms form sheets as shown in Figs. 6(a), (b); the shortest Fe···Fe distance is 8.188 Å for **1** and 8.295 Å for **2** at 90 K. On the other hand, Létard et al. have

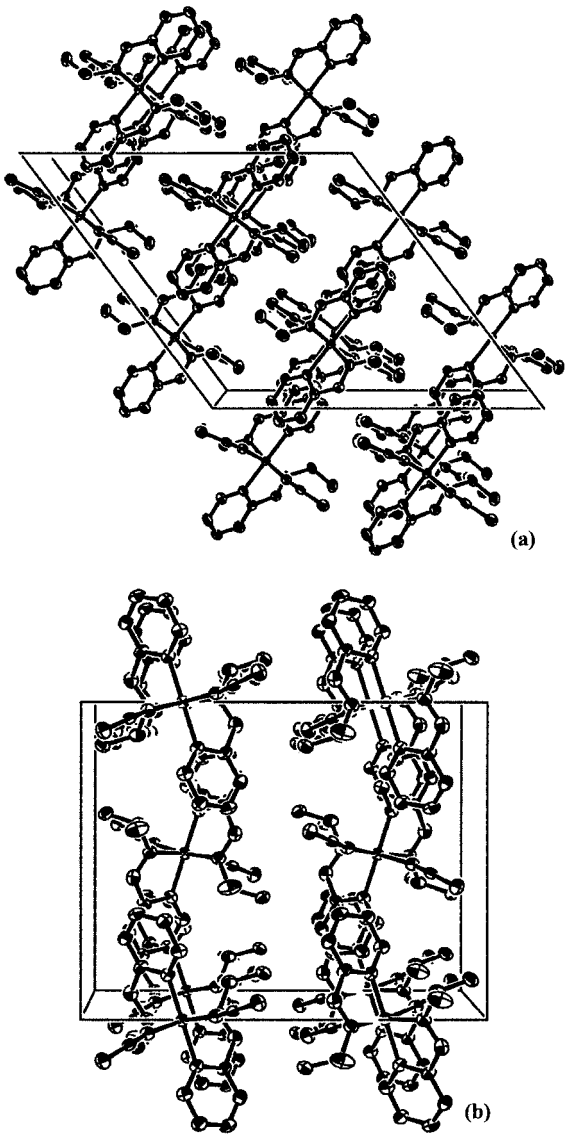

Fig. 6. Crystal packing view of the unit cell along *c* in **1** (a) and **2** (b) at 90 K.

reported that the crystal packing of the compounds **3** and **4** is very tight because of the strong π–π intermolecular interaction between the π system ligands (PM-AzA).[6–8,10] The packing is so close that the shortest Fe···Fe distance is 8.403 Å for **3** and 8.465 for **4** at 90 K despite the much larger ligands. The absence of strong intermolecular interactions in compounds **1** and **2** can explain the inactivity of the photomagnetic interaction; the compounds **1** and **2** with no strong intermolecular interaction do not exhibit LIESST effect, while the compounds **3** and **4** having strong interaction do exhibit the LIESST effect.

The strong cooperative behaviour influences the temperature dependence of the spin-transition behaviour;[19] therefore, a simple model was used to estimate the strength of the intermolecular interactions obtained from magnetic susceptibility data. The values of magnetic susceptibility can be expressed as sums of the magnetic susceptibility of the LS and the HS fractions. In the low temperature region, the magnetic susceptibility of the spin-crossover compounds is not equal to zero,

Table 3. The Thermodynamic Parameters Obtained by Simulating the Data to the Model

	1	**2**	**3**	**4**
ΔH (kJ mol^{-1})	9.6	14.8	4.1	5.5
ΔS (J K^{-1} mol^{-1})	34.7	39.4	21.0	19.81
$T_{1/2}$ (K)	276.3	371.9	202.6	279.5
C	0.58	0.54	0.55	0.69

due to a small paramagnetic contribution of unconverted HS iron(II) ions in addition to some diamagnetic background. If one elevates the temperature, the proportion of HS iron(II) increases until the complete conversion to HS state occurs; therefore, the magnetic moment at high temperature is equal to that of HS iron(II). The temperature dependence of $\chi_m T$ in LS and HS states (e.g. due to zero field splitting) was neglected, and the magnetic behavior above 100 K was considered for the fitting process. The model we used is the regular solution model,[10,20] which in equilibrium leads to the following implicit equation:

$$\ln\left(\frac{1-\gamma_{HS}}{\gamma_{HS}}\right) = \frac{\Delta H_{HL} + \Gamma(1-2\gamma_{HS})}{RT} - \frac{\Delta S_{HL}}{R} \qquad (1)$$

Here, γ_{HS} is a HS fraction, ΔH_{HL} is the enthalpy and ΔS_{HL} is the entropy change associated with the spin transition. The model quantifies the intermolecular interactions by one parameter, Γ. When Γ is smaller than a threshold value equal to $2RT_{1/2}$ ($\Gamma < 2RT_{1/2}$), the transition is gradual; for $\Gamma = 2RT_{1/2}$, the transition curve becomes steep around a transitional temperature; for $\Gamma > 2RT_{1/2}$, a hysteresis appears. Based on the fact that the ratio of Γ to $T_{1/2}$ is more important than the value of Γ itself, Letard et al. introduced a cooperativity factor, which is defined as a convenient parameter $C = \Gamma/2RT_{1/2}$, to compare the intermolecular interactions for different compounds.[10] Since the correlations between these thermodynamic parameters are strong, the results should be discussed with critics. The calculated parameters for the compounds are presented in Table 3 and the fitting curves in Fig. 3. The entropy change of transitions is rather constant, since its main source is the electronic and low-frequency vibrational contributions of the [FeN_6] core; due to the obvious structural similarities these contributions are similar in all the four complexes. There are many factors that can tune the enthalpy change of spin transition ΔH over a wide range of values, which means that the transition temperature is determined mostly by enthalpic factors. The cooperativity of the spin states and the entropy of the transition influence the steepness of the transition. Since the entropy contribution is practically the same for all the complexes **1**–**4**, the cooperativity factor is mainly responsible for the different types of thermal behavior of the studied materials.

Conclusion

The iron(II) compounds **1** and **2** exhibit spin-crossover behaviour. The crystal structures of **1** and **2** were determined at 90 K and 298 K. The crystal packing shows no evidence of strong intermolecular interaction, due to the bulky substitute of the ligand. The compounds **1** and **2** do not exhibit LIESST effect. By contrast, due to the strong intermolecular π–π stacking in the crystals, the compounds **3** and **4** exhibit LIESST effect, as Létard et al. have reported.[6–8,10] The magnitude of intermolecular interactions for the compounds **1**–**4** was estimated by using Eq 1. The obtained cooperativity parameters suggest that both the value of the C and the origin of the cooperativity are important. For compounds **1** and **2**, the cooperative behavior is a result of the elastic interactions; there are no other strong intermolecular interactions, as the packing structure proved. For compounds **3** and **4**, the cooperative behavior is mainly a result of the strong intermolecular π–π stacking interactions. This stacking may distort not only the breathing mode in the [FeN_6] core but other modes, too. Finally, we concluded that the strong intermolecular interactions will play an important role in photo-switchable compounds.

We thank Prof. T. Shinmyouzu (Kyushu Univ.) for use of the X-ray diffractometer (Rigaku IP RAPID). This work was supported by Grants-in-Aid for Science Research (No. 13740400 and 13440197) and for Priority Areas (417) from the Ministry of Education, Culture, Sports, Science and Technology (MEXT), and the Kurata Foundation.

References

1 a) H. A. Goodwin, *Coord. Chem. Rev.*, **18**, 293 (1976). b) P. Gütlich, *Struct. Bonding (Berlin)*, **44**, 83 (1981). c) P. Gütlich and A. Hauser, *Coord. Chem. Rev.*, **97**, 1 (1990). d) E. König, *Prog. Inorg. Chem.*, **35**, 527 (1987). e) E. König, *Struct. Bonding (Berlin)*, **76**, 51 (1991). f) Y. Maeda and Y. Takashima, *Comments Inorg. Chem.*, **7**, 41 (1988). g) J. Zarembowitch, *New J. Chem.*, **16**, 255 (1992).

2 S. Decurtins, P. Gütlich, C. P. Köhler, H. Spiering, and A. Hauser, *Chem. Phys. Lett.*, **105**, 1 (1984).

3 S. Decurtins, P. Gütlich, K. M. Hasselbach, A. Hauser, and H. Spiering, *Inorg. Chem.*, **24**, 2174 (1985).

4 P. Gütlich, A. Hauser, and H. Spiering, *Angew. Chem., Int. Ed. Engl.*, **33**, 2024 (1994).

5 T. Buchen, P. Gütlich, and H. A. Goodwin, *Inorg. Chem.*, **33**, 4573 (1994).

6 J.-F. Létard, P. Guionneau, E. Codjovi, O. Lavastre, G. Bravic, D. Chasseau, and O. Kahn, *J. Am. Chem. Soc.*, **119**, 10861 (1997).

7 J.-F. Létard, P. Guionneau, L. Rabardel, J. A. K. Howard, A. E. Goeta, D. Chasseau, and O. Kahn, *Inorg. Chem.*, **37**, 4432 (1998).

8 J. F. Létard, L. Capes, G. Chastanet, N. Moliner, S. Létard, J.-A. Real, and O. Kahn, *Chem. Phys. Lett.*, **313**, 115 (1999).

9 J.-F. Létard, J. A. Real, N. Moliner, A. B. Gaspar, L. Capes, O. Cador, and O. Kahn, *J. Am. Chem. Soc.*, **121**, 10630 (1999).

10 L. Capes, J.-F. Létard, and O. Kahn, *Chem. Eur. J.*, **6**, 2246 (2000).

11 A. Hauser, P. Gütlich, and H. Spiering, *Inorg. Chem.*, **25**, 4245 (1986).

12 A. Hauser, *J. Chem. Phys.*, **94**, 2741 (1991).

13 R. H. Herber and L. M. Casson, *Inorg. Chem.*, **25**, 847 (1986).

14 R. H. Herber, *Inorg. Chem.*, **26**, 173 (1987).

15 S. Marcén, L. Lecren, L. Capes, H. A. Goodwin, and J.-F. Létard, *Chem. Phys. Lett.*, **358**, 87 (2002).

16 A. Hauser, *Coord. Chem. Rev.*, **111**, 275 (1991).

17 S. Hayami, Z. Z. Gu, M. Shiro, Y. Einaga, A. Fujishima, and O. Sato, *J. Am. Chem. Soc.*, **122**, 7126 (2000).

18 S. Hayami, Z.-Z. Gu, Y. Einaga, Y. Kobayashi, Y. Ishikawa, Y. Yamada, A. Fujishima, and O. Sato, *Inorg. Chem.*, **40**, 3240 (2001).

19 S. Hayami, Z.-Z Gu, H. Yoshiki, A. Fujishima, and O. Sato, *J. Am. Chem. Soc.*, **123**, 11644 (2001).

20 C. P. Slichter and H. G. Drickamer, *J. Chem. Phys.*, **56**, 2142 (1972).